FLOMEKO 2022

The City Gas Flow Standard Facility within (2~4) MPa

Han Zhang[1,2], Liang Wang [1,2], Xinli Dong [1,2*], Donghong Huang[1,2], Peijuan Cao[3*], Yong Li [1,2], Ronghui Shang[1], Shihui Zeng[1], Xuejian Li[1]

[1] Beijing Gas Group Company Limited, 100035, Beijing, China
[2] National City Gas Flowrate Metering Station, 100035, Beijing, China
[3]School of college of career technology, Hebei normal university, Shijiazhuang, Hebei, 050024, China
E-mail (corresponding author): Charles.dongxl@outlook.com; caopj@hebtu.edu.cn

Abstract
In order to meet the traceability requirements of city gas flow meters, the city gas flow standard facility was built based on master meter method. As the non-fixed usage of master meters and the low temperature of natural gas, the uncertainty evaluation and control of the standard facility were investigated. The results showed that the standard facility used four turbine flowmeters as master meters and has mobility, while the achievable flowrate range is within (60~8600) m^3/h and the pressure range of (2~4) MPa. The uncertainty of the non-point usage of the master meters was controlled based on the curve fitting method, while the uncertainty of the city gas flow standard facility was 0.26% (k=2). Compared with NIM-2014, NIM-2015 was more suitable for master meters with scattered error curves. On this basis, the heat transfer model of the cryogenic natural gas flow in pipeline was established. It was found that the dynamic temperature balance of the facility can be achieved through a longer pre-flow time, which can improve the measurement repeatability. The uncertainty of the calibrated flowmeter is 0.32% (k=2). In addition, the comparison experiment with NIM verified the above results.

1. Introduction

The coal is the main primary energy source in China, which takes about 56% among all the primary energy consumption in 2021. Due to the implementation of the carbon peak and neutrality targets and the heavy air pollution resulted from the combustion of coal, the natural gas was more and more widely utilized in China. The total consumption was 320 billion m^3 in 2020, of which city gas accounted for 35.6%. City gas has become one of the main areas of natural gas consumption in China [1].

With the fast development of natural gas, the requirement on the calibration for the natural gas flowmeter was increased for the fair of the trade, especially for the city gas field. It needs the support of accurate measurement of flowmeter, and the accurate measurement of flowmeter depends on the natural gas flow standard facility. According to the verification scheme of measuring instruments for gas flow in China, the natural gas flow standard facility can generally be divided into three categories: primary standard, secondary standard and working standard [2]. The primary standard facility is the source of natural gas flow value traceability. China has built primary standard facilities in Chengdu, Nanjing and Wuhan, and several sets of secondary standard facilities and working standard facilities in Guangzhou, Beijing, Shenyang, Guiyang, Urumqi and other places, which together constitute the magnitude transfer system of gas flow in China [3].

The city gas pressure is generally lower than 4 MPa in China, and the actual working pressure of existing natural gas standard facilities are generally higher than 4 MPa, which cannot effectively meet the high accurate calibration for the city gas flowmeters until now. As the largest single city gas supplier in China, there were only atmospheric pressure air facility before 2019 in Beijing Gas Group Company Limited. In order to improve the calibration ability of domestic city gas flowmeter, the National City Gas Flowrate Metering Station (NCGM) in China was approved to be established and the designing of city gas flow standard facility in NCGM was started in 2019, which was based on Beijing Gas. With consideration of the actual conditions of the gas source, the upper and lower limits of the pressure of the standard were 4 MPa and 2MPa respectively.

In this paper, the detailed information the city gas flow standard will be presented, including the structure of the facility, the uncertainty evaluation and the comparison between the standard facility and the high pressure gas flow standard facility in the national institute of metrology of China (NIM) to verify the uncertainty.

2. The city gas flow standard facility

To meet the requirement of the city gas flowmeter in application, the standard facility was built as the working standard. It used 4 sets of turbine flowmeters with different diameters as the master meter. The achievable flowrate range is within (60~8600) m^3/h and the pressure range of (2~4)

MPa, with the expected best measurement capabilities 0.32% (k=2). As shown in Figure 1, the standard facility was mainly composed of gas source, standard part and working part.

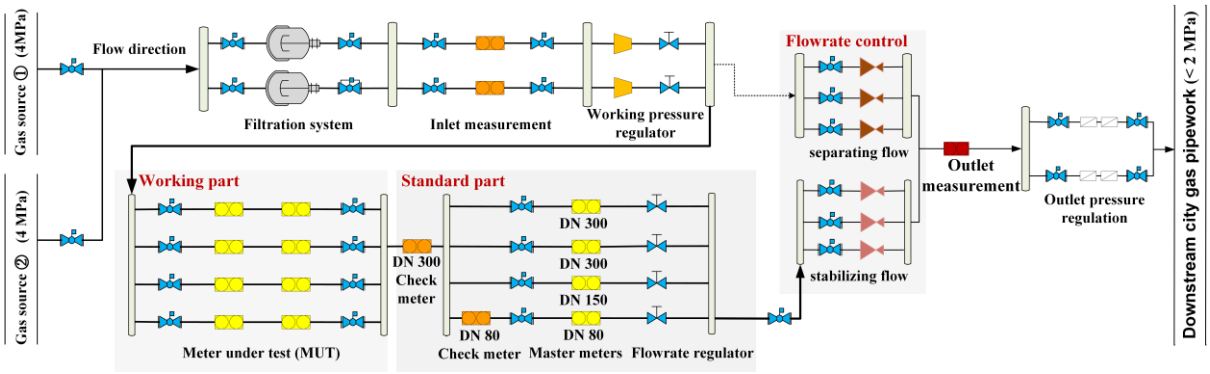

Figure 1: The systematic diagram of the city gas flow standard facility.

- The facility was an open circuit system, and the key to its stable and efficient operation was the gas source. Relying on the city gas pipe network, the standard facility was equipped with two gas sources (as shown in Figure 1). The stability of the gas source was achieved through the stable city gas pipe network. The pressure of the standard facility was continuously adjustable within the range of (2~4) MPa.
- The facility used the multi-stage coupling flowrate control strategy including separating flow, regulating flow and stabilizing flow to the expected flowrate required for the experiment. The flowrate was continuously adjustable within the range of (60~8600) m^3/h.
- In order to meet the needs of on-site calibration of city gas flowmeters, the standard part was skid mounted on the mobile vehicle. It was connected with other parts by flanges, and can complete the calibration on the site with gas source and connection conditions.

3. Uncertainty evaluation for reference flowrate

Based on the conservation of mass, the reference volumetric flowrate through the meter under test (MUT) can be expressed:

$$Q_{v,MUT} = \frac{N_1}{K_{1,C}t} \cdot \frac{p_1}{p_{MUT}} \cdot \frac{T_{MUT}}{T_1} \cdot \frac{Z_{MUT}}{Z_1} . \quad (1)$$

Where, $Q_{v,MUT}$ is the real volumetric flowrate of the MUT; N_1 is the pulse number of the MUT; $K_{1,C}$ is the real meter factor of the master meter; t is the test time; p is the pressure; T is the temperature; Z is the compressibility factor. The subscript of "ref" referring the reference meter, while "MUT" referring the meter under test.

So, the uncertainty of $Q_{v,MUT}$ can be expressed as,

$$u_r(Q_{v,MUT}) = \left\{ \begin{array}{l} u_r(K_{1,C})^2 + u_r(p_1)^2 + u_r(p_{MUT})^2 \\ + u_r(T_1)^2 + u_r(T_{MUT})^2 + u_r(N_1)^2 \\ + u_r(t)^2 + u_r\left(\frac{Z_{MUT}}{Z_1}\right)^2 \end{array} \right\}^{0.5} . \quad (2)$$

The components of natural gas in the MUT and the master meter were approximately the same, the uncertainty introduced by the compressibility factor can be ignored. The uncertainty introduced by the meter factor of the master meter was the main source [4]. This section discussed it in detail.

The 4 sets of turbine flowmeters (DN80, DN150, DN 300-1, DN 300-2) were traceable to the high pressure natural gas flow secondary standard facility in Chengdu. According to the calibration results, the standard uncertainty of master meters was 0.095%, while it used at fixed usage with the same calibration conditions. However, the master meters were commonly used at non-fixed usage in practical applications. The meter factor of master meter with non-fixed usage was calculated by linear interpolation or nonlinear curve fitting based on the calibrated results. Therefore, the uncertainty of the master meter included fixed calibration and non-fixed usage. It has been proved that the nonlinear curve fitting method was suitable for turbine flowmeter with non-fixed usage, especially for working conditions with pressure and temperature changes [5].

The nonlinear curve fitting model NIM-2014 and NIM-2015 were proposed by NIM, which can be expressed as Equ. (3) and Equ. (4) respectively. To cover the calibration flowrate range and pressure range, the curve fitting between error, instead of meter factor, and Reynolds number was made for non-fixed usage of turbine flowmeter.

$$K_{1,C} = a_0 + a_1[\ln(\mathrm{Re})]^1 + a_2[\ln(\mathrm{Re})]^2 + a_3[\ln(\mathrm{Re})]^{-1} + a_4[\ln(\mathrm{Re})]^{-2} . \quad (3)$$

$$K_{1,C} = a_0 + a_1[\ln(\mathrm{Re})]^1 + a_2[\ln(\mathrm{Re})]^2 + a_3[\ln(\mathrm{Re})]^{-1} + a_4[\ln(\mathrm{Re})]^{-2} + \frac{a_5}{\rho Q_{v,1}} \quad (4)$$

Where, Re is the Reynolds number of the master meter; a_0、a_1、a_2、a_3、a_4、a_5 are constant; ρ is the natural gas density of the master meter; $Q_{v,1}$ is the volumetric flowrate of the master meter.

According to Equ. (3) and Equ. (4), the fitting residual calculated respectively, and the model with the minimal fitting residual was selected. Each master meter was calibrated at 2 pressures, ie, 2 Pa and 3.7 MPa. For each pressure, it was calibrated with 8 flowrates. The calculated fitting residual and the fitting results were shown in Table 1 and Figure 2 respectively.

Table 1: Nonlinear fitting residuals of reference meter

	Dn 80	Dn 150	Dn 300-1	Dn 300-2
NIM-2014	0.047%	0.180%	0.076%	0.030%
NIM-2015	0.035%	0.051%	0.049%	0.028%

It was found that the maximum fitting residual of the other three master meters based on NIM-2014 was 0.076%, and the maximum fitting residual based on NIM-2015 was 0.051%, except for DN 150 master meter. It indicated that the fitting residuals of the two models were similar. For the DN 150 master meter, the maximum fitting residual of NIM -2014 was 0.180%, which was about 0.13% higher than NIM-2015.

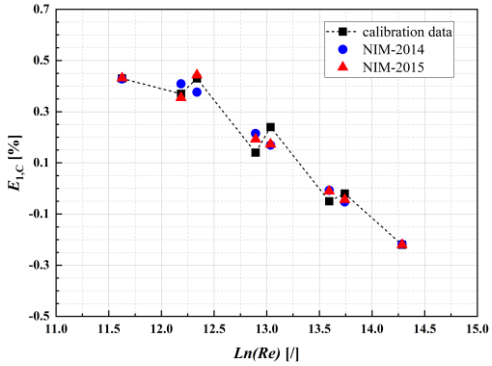

(a) Dn 80

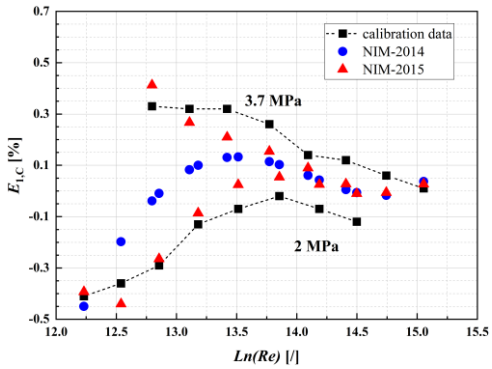

(b) Dn 150

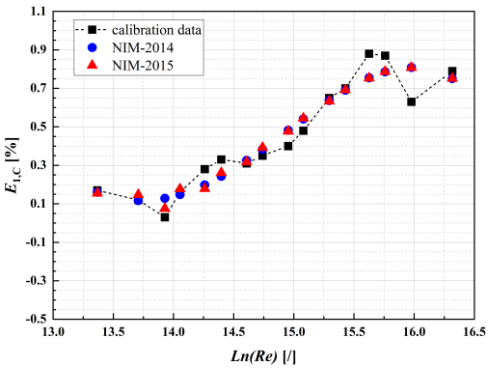

(c) Dn 300-1

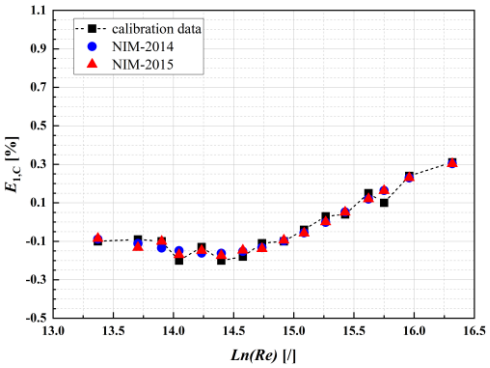

(d) Dn 300-2

Figure 2: Calibration and fitting results of 4 master meters.

For DN 150, the pressure decreased caused the change of Reynolds number, while the error curve dispersed with the decrease of Reynolds number. The dispersion of error curve was more obvious at lower pressure or lower flowrate. For the other master meters, the one-to-one correspondence between the error and the Reynolds number was clearer, which is related to the characteristics of the turbine flowmeter and the reason for optimizing the nonlinear fitting model [6].

Compared with NIM-2014, NIM-2015 can better reflect the error characteristics of turbine flowmeter. When the dispersion of error curve was not obvious, both models can effectively control the uncertainty introduced by the non fixed usage. In this paper, NIM-2015 was used, and the maximum fitting residual of the master meters based on NIM-2015 was 0.051%. So, the uncertainty introduced by the meter factor of the master meter was,

$$u_r(K_{1,C}) = \sqrt{u_r(K_{1,C,C})^2 + u_r(K_{1,C,F})^2} = \sqrt{0.095^2\% + 0.051^2\%} = 0.22\% \quad (5)$$

The detailed uncertainty component of city gas flow standard facility was shown in Table 2. The total uncertainty of $Q_{v,MUT}$ was 0.26% (k=2).

Table 2: The uncertainty component of the reference flow provided by the city gas flow facility

SN	Symbols	Meaning	$c_r(x_i)$	$u_r(x_i)$	$u_r(x_i)\cdot c_r(x_i)$
			[/]	[%]	[%]
1	$u_r(K_{1,C})$	The meter factor of master meter	1	0.22	0.22
2	$u_r(p_1)$	The pressure of master meter	1	0.0289	0.0289
3	$u_r(p_{MUT})$	The pressure of MUT	1	0.058	0.058
4	$u_r(T_1)$	The temperature of master meter	1	0.0098	0.0098
5	$u_r(T_{MUT})$	The temperature of MUT	1	0.0098	0.0098
6	$u_r(N_1)$	The pulse number of master meter	1	0.0058	0.0058
7	$u_r(t)$	The time	1	0.0058	0.0058
$u_r(Q_{v,MUT})$=0.13%, $U_r(Q_{v,MUT})$=0.26%（k=2）					

3. Influence of heat exchange

Further considering the meter factor of MUT, the uncertainty of the meter factor of MUT calibrated by the facility can be expressed as,

$$u_r(K_{MUT,C}) = \sqrt{\begin{matrix} u_r(Q_{v,MUT})^2 + u_r(N_{MUT})^2 \\ +u_r(t)^2 + u_R(K_{MUT,C})^2 \end{matrix}} \quad (6)$$

Where, N_{MUT} is the pulse number of MUT. The uncertainty of measurement repeatability $u_R(K_{MUT,C})$ was easily affected by the temperature stability, which was mainly related to the heat exchange.

In China, natural gas is mostly transported over long distances under high pressure of more than 10 MPa, which far exceeds the maximum design pressure of city gas pipe network. High pressure natural gas needs to reduce pressure before entering the pipeline network. In this process, the expansion and depressurization of natural gas were accompanied by significant temperature drop, which made it actually become a cryogenic fluid. Previous studies have shown that the natural gas temperature could drop by about 50 ˚C when the pressure reduces rapidly from 10 MPa to 4 MPa [7]. The gas source of the facility was close to the upstream gate station, and the natural gas was generally stable below 0 ˚C before entering the facility which was significantly lower than the ambient temperature. The natural gas will continue to exchange heat with the external environment during the experiments.

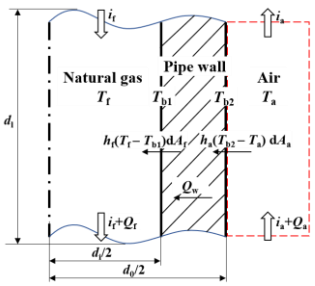

Figure 3: Simplified heat transfer model for low temperature natural gas flow in pipeline

The heat exchange of the facility can be abstractly simplified into three processes, which was shown in Figure 3.

(1) Heat exchange between the outer wall and air. This process included natural convection heat transfer and radiation heat transfer. Assume that the radiation coefficient of ash body is C, the air temperature was Ta. when the outer wall of the pipe temperature $T_{b2}\leqslant 150$, the natural convection heat transfer coefficient h_T and radiation heat transfer coefficient h_R can be expressed as [8],

$$h_T(T_{b2},\ T_a) = 9.4 + 0.052(T_a - T_{b2}) \quad (7)$$

$$h_R[C,\ (T_{b2},\ T_a)] = C\frac{(\frac{T_{b2}}{100})^4 - (\frac{T_a}{100})^4}{T_a - T_{b2}} \quad (8)$$

The heat transfer rate of air to the outer wall Q_a can be calculated based on the Equ. (9).

$$Q_a = 2\pi d_0 d_1 (h_T + h_R)(T_a - T_{b2}) \quad (9)$$

(2) Heat conduction of the pipe wall. Assuming that the thermal conductivity of the pipe wall was λ_w, the heat transfer rate of the pipe wall Q_w can be expressed as Equ. (10) [9],

$$Q_w = \frac{T_{b2} - T_{b1}}{\ln(d_0/d_i)} 2\pi d_1 \lambda_w \quad (10)$$

(3) Convective heat transfer between the inner wall of the pipe and the natural gas. Assume that the thermal conductivity of natural gas is λ, dynamic viscosity is μ, constant pressure specific heat capacity is C_p, flow velocity is v, natural gas heating and cooling coefficient n are all determined. When Re>10000 and 0.7<P_r<120, the forced convection heat transfer coefficient H_f [10] between the inner wall and natural gas can be expressed as,

$$h_f(\lambda,\ \mu,\ \rho,\ C_p,\ d_i,\ v) = 0.023\frac{\lambda}{d_i}(\frac{d_i v\rho}{\mu})^{0.8}(\frac{C_p\mu}{\lambda})^n \quad (11)$$

Where, the coefficient n is related to the inner wall temperature T_{b2} and the natural gas temperature T_f. The heat transfer rate Q_f from inner wall to the natural gas can be expressed as Equ. (12).

$$Q_f = 2\pi d_i h_f (T_{b1} - T_f) d_l \quad (12)$$

The change of natural gas temperature depended on the heat transfer rate difference of adjacent heat transfer processes, and the heat transfer rate was related to the temperature difference. When the heat transfer was in dynamic equilibrium, the three heat transfer processes were in dynamic equilibrium and each heat transfer rate was equal. At this time, the natural gas temperature T_f can be expressed as,

$$T_f = T_{b2} - [\frac{1}{h_f d_i} + \frac{\ln(\frac{d_0}{d_i})}{\lambda_w}][(h_T + h_R)(T_a - T_{b2})d_0] \quad (13)$$

From Equ. (13), the natural gas temperature during dynamic equilibrium was mainly related to the air temperature and the outer wall temperature under certain working pressure and flowrate. Considering the natural gas, pipe wall and external ambient temperature, the heat transfer process of natural gas passed through non-equilibrium state and dynamic equilibrium state after flowing.

After stopping operating for a long time, the temperature of the pipe wall was approximately equal to the air. When the cryogenic natural gas flowed, the temperature difference between the inner wall and the fluid was maximum, which means that Q_i was maximum at this time and was greater than Q_w and Q_a. With the continuous flow, the inner wall temperature decreased faster than the outer wall, while Q_w and Q_a increased with the decrease of Q_f, and the facility was in a non-equilibrium state. The inner wall temperature as well as the outer wall approached the same with the natural gas as the flow distance increased, which made the heat transfer rate tend to be equal. The facility developed from non-equilibrium state to dynamic equilibrium state.

So, the facility can gradually achieve the dynamic equilibrium state with the increase of flow time controlled by the flow time. The tested results of temperature stability were shown in Figure 4.

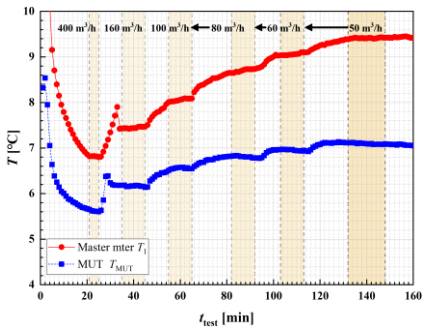

(a) Temperature trend

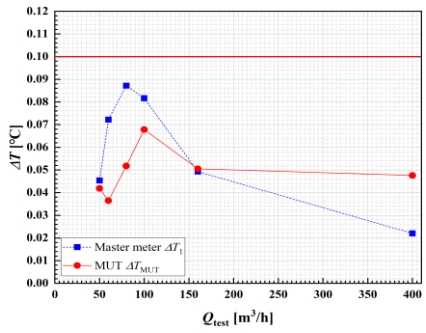

(b) Temperature difference

Figure.4: Experimental results of temperature stability

Based on the temperature control method, a DN 100 turbine flowmeter was used as MUT to carry out the measurement repeatability experiment. The calibration procedure was as follows,

- The MUT was calibrated at 6 pressures, ie, 2 MPa, 2.8 MPa, 3.2 MPa, 3.4 MPa, 3.6 MPa, and 3.8 MPa.
- For each pressure, the meter was calibrated with 7 flowrates, ie, 60 m³/h, 70 m³/h, 80 m³/h, 100 m³/h, 160 m³/h, 240 m³/h, and 400 m³/h.
- For each pressure with different flowrate, the meter was calibrated for 6~10 times as a group, and the repeatability under the working condition was calculated by Equ. (15).

$$u_R(K_{MUT,C}) = \frac{\sqrt{\sum_{i=1}^{n}(k_{MUT,C,i} - \overline{k_{MUT,C,i}})^2}}{\overline{k_{MUT,C,i}}} \times 100\% \quad (14)$$

$$\overline{k_{MUT,C,i}} = \frac{1}{n}\sum_{i=1}^{n} k_{MUT,C,i} \quad (15)$$

42 groups of experimental results were shown in Figure 5. The results were all between 0.01% and 0.08%, while it increased significantly with the decrease of pressure and flowrate. Among them, 35 groups were less than 0.07%, accounting for 83.3%. 7 groups were more than 0.07% and all of them were below 2.8 MPa. According to the experimental results, the maximum repeatability was 0.08%, which was used as $u_{R(}K_{MUT,C)}$.

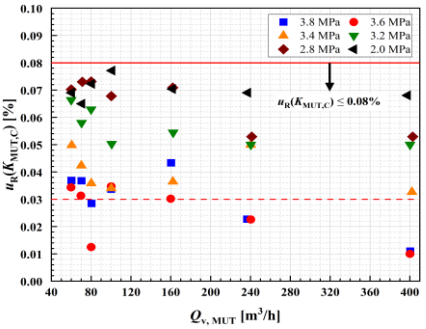

(a)

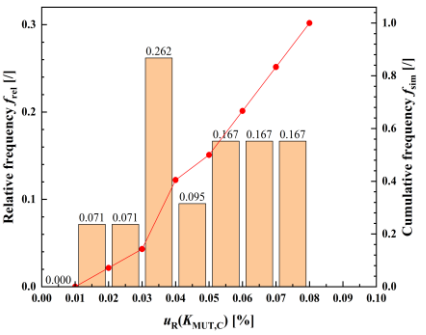

(b)

Figure 5: Experimental results of temperature stability

The detailed uncertainty component of the meter factor of MUT calibrated by the standard facility was shown in Table 3. The total uncertainty of $K_{MUT,C}$ was 0.32% (k=2).

Table 3: The uncertainty component of the calibrated meter factor by the city gas flow facility

SN	Symbols	Meaning	$c_r(x_i)$	$u_r(x_i)$	$u_r(x_i)\cdot c_r(x_i)$
			[/]	[%]	[%]
1	$u_r(Q_{v,MUT})$	The reference flow	1	0.13	0.13
2	$u_r(N_{MUT})$	The pulse number of MUT	1	0.0058	0.0058
3	$u_r(t)$	The time	1	0.002	0.002
4	$u_R(K_{MUT,C})$	The measurement repeatability	1	0.08	0.08
$u_r(K_{MUT,C})$=0.16%， $U_r(K_{MUT,C})$=0.32%（k=2）					

5. The verification on the evaluated uncertainty

To verify the evaluated uncertainty of the city gas flow standard facility, one Dn 200 turbine meter was used as the transfer meter to make the comparison between the facility and the high pressure gas flow standard facility in NIM. Within the overlap region of Reynolds number, the En value [11] was used to evaluate the result. Due to the difference between the comparison experimental results, the measurement results of the standard facility were curve fitted, and the influence of fitting residual was considered in the analysis.

$$E_n = \frac{\left|E_{test,BJ,CF} - E_{test,NIM}\right|}{\sqrt{U^2_{test,BJ} + U^2_{test,NIM} + U^2_{CF}}}. \quad (16)$$

- For city gas facility, the expanded uncertainty of meter factor for meter under test (MUT) is 0.32% (k=2).
- For facility in NIM, the expanded uncertainty of meter factor for meter under test (MUT) is 0.18% (k=2).

The comparison results were shown in Figure 6

.

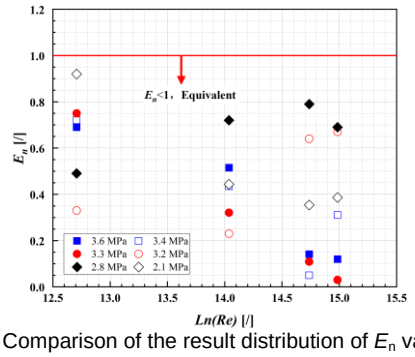

Figure 6: Comparison of the result distribution of E_n values

6. Conclusion

In 2021, the city gas flow standard facility was built in China. Aiming at the problems of non-fixed usage of master meter and cryogenic fluid flow, the uncertainty evaluation and control research were carried out. The results show that:

- The standard facility used 4 sets of turbine flowmeters with different diameters as master meters and has mobility, while the achievable flowrate range was within (60~8600) m^3/h and the pressure range of (2~4) MPa.
- The uncertainty of the non-point usage of the master meters was controlled by curve fitting, while the uncertainty of the city gas flow standard facility was 0.26% (k=2). Compared with NIM-2014, NIM-2015 was more suitable for master meters with scattered error curves.
- The heat transfer model of the cryogenic natural gas flow was established. It was found that the dynamic temperature balance of the facility can be achieved by a longer pre-flow time, which can improved the measurement repeatability. The uncertainty of the calibrated flowmeter is 0.32% (k=2).

References

[1] www.BP.com, BP statistical review of word energy, June, 2021.

[2] Wang C., et. al., The high pressure close loop gas flow standard facility in NIM. Flomeko, Portugal, Lisbon, 2019.

[3] Yang Y. P., et. al., Capacity improvement of natural gas flow standard device. Acta Metrologica Sinica, 2021, 42(03), 339-345.

[4] Ren J., et. al., Application and uncertainty analysis of a new balance used in natural gas primary standard up to 60 bar. Flomeko, Portugal, Lisbon, 2019.

[5] Li C. H., et. al., The investigation on the evaluation for the turbine meter by the use of non-fixed point as master meter, Acta Metrologica Sinica, 2015, 36(6), 610-612.

[6] Zhang H., et. al., The error model of turbine flowmeter based on Reynolds number. Flomeko, Sydney, Australia, 2016.

[7] Li J. J., Cold energy recovery and its applications research of natural gas in the city gate station (Chongqing, Chongqing University) 2011.

[8] Donald Q. K., Process Heat Transfer (New York, Mc-Graw-Hill), 1990.

[9] Garrido P. L, et. al., Simple one-dimensional model of heat conduction which obeys fourier's law. Physical Review Letters, 2001, 86(24), 5486-5489.

[10] Dittus F. W., et. al., Heat transfer in automobile radiators of the tubular type[J]. International Communications in Heat and Mass Transfer, 1985, 28(1), 3-22.

[11] Cox M. G., The evaluation of key comparison data. Metrologia, 2002, 39(6), 589-595.